*Inflammation, Vol. 42, No. 4, August 2019 (© 2019)*
DOI: 10.1007/s10753-019-00998-z

ORIGINAL ARTICLE

# Desmoglein 3 Silencing Inhibits Inflammation and Goblet Cell Mucin Secretion in a Mouse Model of Chronic Rhinosinusitis *via* Disruption of the Wnt/β-Catenin Signaling Pathway

**Jinzhang Cheng,[1] Jingpu Yang,[1] Kai Xue,[1] Yin Zhao,[1] Chang Zhao,[1] Song Li,[1] and Zonggui Wang[1,2]**

*Abstract*— Chronic rhinosinusitis (CRS) is a common disease characterized by inflammation of the nose and paranasal sinuses lasting over 12 weeks. This study aims to evaluate the effect of desmoglein 3 (DSG3) on inflammatory response and goblet cell mucin secretion in a mouse model of CRS. The CRS-related differentially expressed genes and disease genes were screened using microarray-based gene expression analysis. Subsequently, CRS mouse models were established. The levels of pro-inflammatory factors TNF-α, IL-6, and IL-8 were measured by ELISA. In addition, loss-of-function experiment was conducted using siRNAs targeting DSG3 and β-catenin. The secretion of mucins MUC5B and MUC5AC in goblet cells was detected, and the apoptosis of goblet cells was assessed. The regulatory effect of DSG3 on the Wnt/β-catenin signaling pathway was analyzed by determining the mRNA and protein levels of DSG3, Wnt, β-catenin, and GSK3β. DSG3 was identified to be an upregulated gene in CRS, which was further documented in CRS mice models. Elevated inflammation and mucin production were noted in CRS mice models. Also, it was found that DSG3 or β-catenin silencing could decrease the levels of TNF-α, IL-6, and IL-8, and the positive rates of MUC5B and MUC5AC while enhancing goblet cell apoptosis. The Wnt/β-catenin signaling pathway was blocked by DSG3, evidenced by downregulated Wnt and β-catenin as well as upregulated GSK3β mRNA and protein levels. Overall, this study provides evidence that silencing DSG3 could inhibit the activation of the Wnt/β-catenin signaling pathway, thus alleviating CRS.

**KEY WORDS:** desmoglein 3; Wnt/β-catenin signaling pathway; chronic rhinosinusitis; inflammatory response; MUC5B; MUC5AC.

## INTRODUCTION

Chronic rhinosinusitis (CRS) is a complex inflammatory disorder characterized by inflammation of nasal and paranasal sinus mucosa [1]. CRS affects approximately 10% of people in Western countries and is featured by several symptoms such as drainage, facial pressure, persistent nasal obstruction, and loss of smell [2]. Mucin glycoproteins, such as MUC7, belonging to the body's intrinsic immune system, may protect CRS patients against inhalation and ingestion of aeroallergens and pathogens [3]. In addition, genetic or environmental components have been implicated in the pathogenesis of CRS [4]. Although comprehensive investigation efforts for the treatment of CRS have been made in the past, it remains

[1] Department of Otolaryngology Head and Neck Surgery, The Second Hospital of Jilin University, No. 218, Ziqiang Street, Nanguan District, Changchun, 130000, Jilin Province, People's Republic of China
[2] To whom correspondence should be addressed at Department of Otolaryngology Head and Neck Surgery, The Second Hospital of Jilin University, No. 218, Ziqiang Street, Nanguan District, Changchun, 130000, Jilin Province, People's Republic of China. E-mail: w_zonggui@163.com

difficult to specify and identify the roles of anatomic, external, and host immunologic factors in the pathogenic mechanism [5]. A previous study indicated the involvement of a high expression of desmoglein 3 (DSG3) in CRS sinus mucosa in the glandular formation [6]. A comprehensive analysis of DSG3 might be conducive to deeper understudying of the molecular mechanism in CRS.

DSG3 is a keratinocyte cell–cell adhesion molecule that is essential for epidermal integrity and an autoantigen in the autoimmune blistering disease pemphigus [7]. DSG3 is known to mediate cell–cell adhesion and E-cadherin-Src signaling in several skin inflammatory disorders, such as pemphigus vulgaris [8]. As a subset of the cadherin–catenin group, the expression of β-catenin may control cell–cell adhesion, frequently involving in progression [9]. β-catenin is an important regulator of the Wnt pathway for various cellular responses, and acts as transcriptional activator of carcinogenic genes participating in tumorigenesis [10]. Interestingly, it has been revealed that activation of the Wnt/β-catenin signaling pathway reduces the expression of certain mucins, such as MUC5B [11]. In general, activation of the Wnt signaling pathway facilitates the maintenance of the inflammatory state and tissue remodeling of CRS with nasal polyps (CRSwNP), and blocking this pathway may be of therapeutic value for patients with CRSwNP [12]. Furthermore, a complex of DSG3, E-cadherin, β-catenin, and Src was previously proposed to control the desmosome assembly, which is vital for the maintenance of the integrity of cells and tissues [13].

From all the aforementioned findings and evidence, we proposed a hypothesis that DSG3 silencing and inhibition of the Wnt/β-catenin signaling pathway could protect against CRS on the basis of the obtained microarray gene expression profiling. To investigate this hypothesis, the current study aimed to examine the effects of DSG3 and Wnt/β-catenin signaling pathway on inflammatory response and goblet cell mucin secretion in a mouse model of CRS, so as to provide a novel therapeutic target for the treatment of CRS.

## MATERIALS AND METHODS

### Microarray Gene Expression Profiling

The GSE10406 expression datasets and probe annotation files of CRS were obtained from the Gene Expression Omnibus (GEO) database (https://www.ncbi.nlm.nih.gov/geo-/), and the gene annotation platform was GPL570 [HG-U133Porth2] using the Affymetrix Human Genome U133 Plus 2.0 Array. The GSE10406 chip contained the expression data of sinus mucosa of nine normal counterpart and nine patients with CRS. The R language Affy package (http://www.bioconductor.org/package/release/bioc-htmlr/affy.html) was employed to perform the standardized pretreatment of expression data. Differentially expressed genes (DEGs) were screened using the limma package of the R language (http://master.bioconductor.org/packages/release/bioc/html/limma.html) with the screening thresholds of log fold change $>2$ and $p$ val. $<0.05$, and heatmap for DEGs was plotted with the pheatmap package in the R language (https://cran.r-project.org/web/packages/pheatmap/index.html). Subsequently, the genes related to CRS, namely disease genes, were searched from the gene-disease database DisGeNET (http://www.disgenet.org/web/DisGeNET/menu/search?4). The interaction between DEGs and disease genes of CRS was retrieved from the String database (https:/string-db.orgr/) using the Cytoscape 3.6.0 software, and the interaction network was constructed and a functional analysis was carried out.

### Mouse Models of CRS

A total of 65 C57 mice (provided by Model Animal Research center of Nanjing University, Nanjing, Jiangsu, China) aged 6–8 weeks and weighing 18–22 g were selected. The aforementioned mice were fed fine particle with free access to water, natural lighting, and a 12-h light/dark cycle. A total of 10 mice without any treatment were randomly selected as normal group, and the remaining 55 mice were used to establish mouse models of CRS [14]. In brief, the expanded sponge was placed inside the left nasal cavity (about 15 mm from the anterior nares), and infused with droplets of *Staphylococcus aureus*. After the model was established (three mice died during the modeling), 50 modeled mice were assigned into the following five groups (with 10 mice in each group): CRS (mice of CRS model without treatment), negative control (NC) (mice of CRS model injected with empty plasmid), si-DSG3 (mice of CRS model injected with siRNA targeting DSG3), si-β-catenin (mice of CRS model injected with siRNA targeting β-catenin), and si-DSG3 + β-catenin (mice with CRS injected with siRNAs targeting si-DSG3 and si-β-catenin). The transfection solution was prepared as follows: (1) 80 μg of si-RNA powder including si-DSG3 (abx914664, Abbexa, Cambridge, UK) or si-β-catenin (284028-89-3, StemRD, Burlingame, CA, USA) or si-DSG3 (abx914664, Abbexa, Cambridge, UK) + si-β-catenin (284028-89-3, StemRD, Burlingame, CA, USA) was centrifuged, and then fully mixed with 100 μL of 5% glucose solutions. (2) Eight microliter of *in vivo* jetPEITM

(201-10G, Polyplus Battery Co., Berkeley, CA, USA) was fully mixed with 92 μL of 5% glucose solution. A total of 200 μL was cultured for 20 min. The transfection solution was injected into both sides of the mouse nasal cavity, and the nasal cavity was closed with layered sutures. The current study was carried out in accordance with principles for the management and use of local laboratory animals. All efforts were made to minimize the suffering of the included animals.

### Animal Treatment and HE Staining

After transfection for 48 h, the mice were euthanized, and the maxilla was extracted. Next, the nasal septum and bilateral nasal cavity were exposed, and about 8-mm tissue blocks were collected from nasal sinuses and preserved in liquid nitrogen. The tissues were weighed, and 10% homogenate was prepared with the addition of nine-fold normal saline. One part of tissues was centrifuged under 4 °C at 3000 rpm for 10 min; the supernatant was obtained and then frozen at 80 °C. The remaining tissues were fixed with 10% formaldehyde, dehydrated, and embedded with paraffin, and sliced into 4-μm sections for further experimentation.

The paraffin sections were dewaxed two times in xylene (15 min for each), and rehydrated in gradient alcohol (100%, 100%, 90%, and 80%; 5 min for each). After being washed with tap water for 5 min, the sections were stained with hematoxylin for 5 min and washed again. Next, the sections were differentiated in 1% hydrochloric acid alcohol, and then washed again. The sections were then dehydrated with gradient alcohol (80%, 90%, 100%, and 100%; 5 min for each), cleared two times in xylene (15 min each time), and mounted with neutral balsam. Histopathological changes of the tissues were observed and photographed under a microscope (H-7500; Hitachi, Tokyo, Japan). The images (200×) were collected using a JD-801 morphological image analysis (MIA) system (Jiangsu Jeda Science-Technology Development Co., Ltd., Nanjing, Jiangsu, China). Experiments were repeated three times.

### AB-PAS Staining

The mucin granules in goblet cells were tested using Alcian blue-periodic acid-Schiff (AB-PAS) staining [15], according to the specification of the PAS staining Kit (DG0005, Beijing Leagene Biotechnology Co., Ltd., Beijing, China). The paraffin-embedded sections were baked in an incubator at 70 °C for about 90 min until the paraffin melted. After being dewaxed twice with xylene solution (10 min for each), the sections were rehydrated with gradient alcohol (100%, 95%, and 85%; 5 min for each), and then washed under tap water and distilled water. Next, the sections were stained with PAS dye liquor A (1% periodic acid) at room temperature for 6 min, PAS dye liquor B (Schiff dye) for 15 min, and PAS dye liquor C (hematoxylin) for 2 min, and differentiated with PAS dye liquor D (1% hydrochloric alcohol) for 2–3 s. The sections were then rinsed with distilled water to return to blue, with tap water for 13 min, and then washed three times with distilled water (5 min for each). After washing, the sections were dehydrated with gradient alcohol (85%, 95%, 100%, and 100%, 5 min for each), cleared twice with xylene (10 min for each), and air-dried. Finally, the issues were added with a drop of neutral balsam and mounted with a cover glass, and observed under a microscope.

### ELISA

A total of 50 mg tissues was placed into a 2.0-centrifuge tube, and rinsed with 0.05 mmol/L pre-cooled phosphate buffer saline (PBS). After rinsing, the tissues were added with 0.5 mL of pre-cooled PBS, homogenized with a high-speed homogenizer in an ice-bath for 2 min, and centrifuged at 3000 rpm for 10 min at 4 °C. The concentrations of TNF-α, IL-6 and IL-8 in the supernatant were measured according to the instructions of the enzyme-linked immunosorbent assay (ELISA) Kit (69–99,985; 69–99,854; 69–21,138, Wuhan MSK Biotechnology Co., Ltd., Wuhan, Hubei, China). The samples were diluted to appropriate proportions, and 50 μL of standard sample and diluted sample were added to the ELISA plate. After membrane reaction, the solution in the enzyme labeled plate was discarded, and 50 μL of enzyme labeling reagent was added to each well for incubation at 37 °C for 30 min. After incubation, the plate was rinsed three times with phosphate buffered saline (PBS). Subsequently, 50 μL of chromogenic agent A and 50 μL of chromogenic agent B were mixed together in each well, and then the chromogenic reaction was performed at 37 °C in dark conditions for 15 min and terminated with stop buffer. The optical density (OD) values of each well were measured using an excitation wavelength of 450 nm using a microplate reader (Synergy 2, BioTek, Winooski, VT, USA) within 3 min. According to the OD values, we found the corresponding concentration in the standard curve, which was multiplied by dilutability to calculate the final OD values of samples [16, 17].

### Immunohistochemical Staining

The following steps were conducted according to the specifications of the immunohistochemical staining kit (SPM120, MRbiotech Co., Ltd., Shanghai, China). After

dewaxing and antigen retrieval, the paraffin-embedded sections were soaked in 3% $H_2O_2$-methanol for 10 min to remove the endogenous peroxidase, followed by rinsing with PBS. Next, the sections were incubated with a drop of normal goat serum for 10 min. The sections were then incubated with the primary antibody, the mouse polyclonal antibody to MUC5B (ab77995) and MUC5AC (ab24071) in a wet box for 30–60 min, followed by PBS rinsing. Following that, the sections were stained with one drop of the secondary antibody, the biotin-labeled goat anti-rabbit antibody to immunoglobulin G (IgG; ab205718) or goat anti-mouse IgG (ab205719) for 10 min, followed by PBS rinsing. All aforementioned antibodies were purchased from Abcam Inc. (Cambridge, MA, USA). After that, the sections were incubated with a drop of streptavidin-conjugated horseradish peroxidase (Beijing Zhongshan Golden Bridge Biotechnology Co., Ltd., Beijing, China) for 10 min, followed by PBS rinsing. Subsequently, the sections were dropped with diaminobenzidine (DAB) for developing for 2–5 min at room temperature. The sections were then counterstained with hematoxylin, and differentiated in 0.1% hydrochloric acid alcohol. After dehydration, clearing, and sealing, the sections were observed under a microscope. Instead of the primary antibody, PBS was used as the NC, and normal mucosa as a positive control. A total of five positive visual fields (400×) were randomly selected from each section, and 100 cells in each field were counted. The percentage of positive cells was scored as follows [18]: positive cells/total cells > 10% was recorded as positive (+), and positive cells/total cells ≤ 10% was negative (−).

## TUNEL Assay

A total of 5 above dewaxed sections were collected and added with 50 μL of 1% proteinase K diluent. Next, the sections were incubated for 30 min in a thermostat at 37 °C, and rinsed 3 times in PBS (5 min for each). The sections were then added with 0.3% $H_2O_2$ methanol solution to eliminate the endogenous peroxidase, incubated at 37 °C for 30 min and rinsed three times in PBS (5 min for each). After rinsing, the sections were added with terminal deoxynucleotidyl transferase (TdT)-mediated dUTP nick-end labeling (TUNEL) reaction solution, placed in a wet box at 37 °C for 1 h and rinsed three times with PBS (5 min for each). After that, the sections were added with 50 μL of converter-peroxidase, incubated at 37 °C in a wet box for 30 min, and rinsed three times with PBS (5 min for each). Then, the sections were added with 2% DAB developing solution and incubated for 15 min at room temperature. Under microscopic observation, the cells presented with brown nuclei, and then were added with distilled water to terminate the reaction. Following termination, the sections were rinsed three times with PBS (5 min for each), washed one time with distilled water, incubated for 3 min in 3% glacial acetic acid solution at room temperature, and rinsed under tap water for 2 min. After being washed one time with the distilled water, the sections were stained with Alcian blue dye for 30 min and washed under tap water for 1 min. The nucleus was stained with hematoxylin for 32 s and differentiated for 3 s in hydrochloric acid. After staining, the sections were rinsed under tap water to return to blue, dehydrated with absolute alcohol, cleared with xylene, and sealed in neutral balsam.

## RT-qPCR

The total ribonucleic acid (RNA) content from the sinus mucosa tissues of the mice was extracted according to the instructions of a TRIzol reagent (Invitrogen Company, Carlsbad, CA, USA). The obtained RNA was diluted with ultrapure water containing diethyl pyrocarbonate (DEPC). The OD values of the RNA samples were measured at excitation wavelengths of 260 nm, and 280 nm were measured using a Biochrom Ultrospecultra violet/visible light spectrophotometer (Biochrom Company, Cambridge, UK), and subsequently, the purity and integrity of total RNA were determined. The primers of DSG3, β-catenin, Wnt, and Glycogen synthase kinase-3β (GSK3β) were designed and synthesized by Nanjing GenScript Biotechnology Co., Ltd. (Nanjing, Jiangsu, China) (Table 1), with β-actin serving as the internal reference. Reverse transcription (20 μL) was conducted according to the instructions of TaqMan MicroRNA Assays Reverse

**Table 1.** Primer sequence for RT-qPCR

| Gene | Primer sequence |
|---|---|
| DSG3 | F: 5′-GGAGGAACAGACTAACAGGC-3′ |
| | R: 5′-ACCATCAGGAGGGCCAGAGA-3′ |
| Wnt | F: 5′-CCATGAACCGTCACAACAATGAG-3′ |
| | R: 5′-CACCAGCAGGTCTTCACTTCACA-3′ |
| β-catenin | F: 5′-CTTCATTATGGATGCCTGTTGTG-3′ |
| | R: 5′-TGGGTGTCCTGATGTGCTCG-3′ |
| GSK3β | F: 5′-CTGCTTCTCCCGGTATTGTTTTG-3′ |
| | R: 5′-CTGCCACCTTCCTGTTCTTCG-3′ |
| β-actin | F: 5′-CACGATGGAGGGGCCGGACTCATC-3′ |
| | R: 5′-TAAAGACCTCTATGCCAACACAGT-3′ |

*F* forward, *R* reverse, *DSG3* desmoglein 3, *GSK3β* glycogen synthase kinase-3β, *RT-qPCR* reverse transcription quantitative polymerase chain reaction

Transcription Primer (4,366,596, Thermo Fisher Scientific Inc., Waltham, MA, USA), and the reactions were as follows: reverse transcription reaction was carried out at 42 °C for 30–50 min, and reverse transcription inactivation reaction at 85 °C for 5 s. Reverse transcription quantitative polymerase chain reaction (RT-qPCR) was performed according to the instructions of SYBR® Premix Ex TaqTM II Kit (RR820A, Xingzhi Biotechnology Co., Ltd., Guangzhou, Guangdong, China). The reaction system (total of 50 μL) included 25 μL of SYBR® Premix Ex Taq™II (2×), 2 μL of forward primers and 2 μL of reverse primers, l μL of carboxyl-X-rhodamine (ROX) reference dye (50×), 4 μL of deoxyribonucleic acid (DNA) template, and 16 μL of $ddH_2O$. RT-qPCR was conducted with using an ABI PRISM® 7300 (Prism® 7300, Shanghai Kunke Instrument and Equipment Co., Ltd., Shanghai, China). The reaction conditions were as follows: pre-denaturation at 94 °C for 10 min, and a total of 40 cycles of denaturation at 94 °C for 15 s, annealing at 55 °C for 30 s, and extension at 72 °C for 1 min. The reliability of the PCR reactions was evaluated using the melting curve analysis. The threshold cycle (Ct) values were set, and the relative expression of the target gene was calculated based on the $2^{-\Delta\Delta Ct}$ method, in which $\Delta Ct$ = Ct (target gene)—Ct (internal reference) and $\Delta\Delta Ct = \Delta Ct$ (experiment group)—$\Delta Ct$ (control group). Each experiment was performed in triplicates to obtain the mean value.

### Western Blot Analysis

A total of 25 mg of sinus mucosa tissues was rinsed with PBS solution to remove the surface impurities of the tissues. The tissues were dried and placed into a homogenizer, and then added with about 500 μL of radio immunoprecipitation assay (RIPA) lysis buffer, followed by homogenization for 20–30 times. Next, the tissues were transferred to a 1.5-mL Eppendorf (EP) tube, lysed on ice for 20–30 min, centrifuged at 25764–35068 g for 5 min at 4 °C. The obtained supernatant was transferred into an EP tube. Subsequently, a bicinchoninic acid (BCA) protein quantitative kit (No. 23228, Thermo Fisher Scientific Inc., Waltham, MA, USA) was used to determine the protein concentration of the tissues. The protein sample was separated using sodium dodecyl sulfate-polyacrylamide gel electrophoresis (SDS-PAGE), transferred onto a poly-vinylidene fluoride (PVDF) membrane for 90 min at 90 V constant pressures, stained with Ponceau S for 3–5 min to observe the protein bands. The membrane was immersed in Tris-buffer saline with Tween (TBST) for 3–5 min to remove ponceau S, and then blocked in 5% skim milk powder for 1 h. Then, the membranes were incubated with the primary antibody, the rabbit anti-mouse antibody to DSG3 (dilution ratio of 1:500, ab203692), the rabbit anti-mouse antibody to Wnt (dilution ratio of 1:1000, ab15251), the rabbit anti-mouse antibody to β-catenin (dilution ratio of 1:5000, ab32572), the rabbit anti-mouse antibody to GSK3β (dilution ratio of 1:5000, ab32391) and rabbit anti-mouse β-actin (dilution ratio of 1:5000, ab8227) at 4 °C overnight. The membranes were washed three times with TBST times (15 min for each). Next, the membranes were incubated with the secondary antibody, horseradish peroxidase (HRP)-labeled goat anti-rabbit to IgG (ab205718, dilution ratio of 1:3000) at 4 °C for 1 h, and washed three times with TBST (15 min for each). All aforementioned antibodies were purchased from Abcam Inc. (Cambridge, MA, USA). Finally, the membranes were incubated in the developer at room temperature for 3 min, and then the developer was removed, followed by fixing the membrane, exposure to X-ray, and visualization. β-actin was served as the internal reference. The protein relative expression of target gene was calculated by the ratio of the gray value of the target gene and the internal inference.

### Statistical Analysis

Statistical analyses were performed using the SPSS 19.0 software (IBM Corp. Armonk, NY, USA). Measurement data were presented as mean value ± standard deviation. The *t* test was applied for comparisons between two groups. Data that did not conform to heterogeneity of variance were corrected using Welch's. Comparisons among multiple groups were analyzed using one-way analysis of variance (ANOVA), and pairwise comparison was examined using the Tukey *post hoc* test. Non-parametric test was performed for data with skewed distribution for pairwise comparison. A value of $p < 0.05$ was considered to be statistically significant.

## RESULTS

### DSG3 Is Expressed at a High Level in CRS

Initially, the R language was used to screen DEGs from the CRS-related gene expression chip GSE10406, with $|\log2FC| > 2.0$ and adj. $p$ val. $< 0.05$ serving as the threshold. Subsequently, the heatmap of the top 20 DEGs was plotted as shown in Fig. 1a. The CRS-related genes were searched using the DisGeNET database, and the top

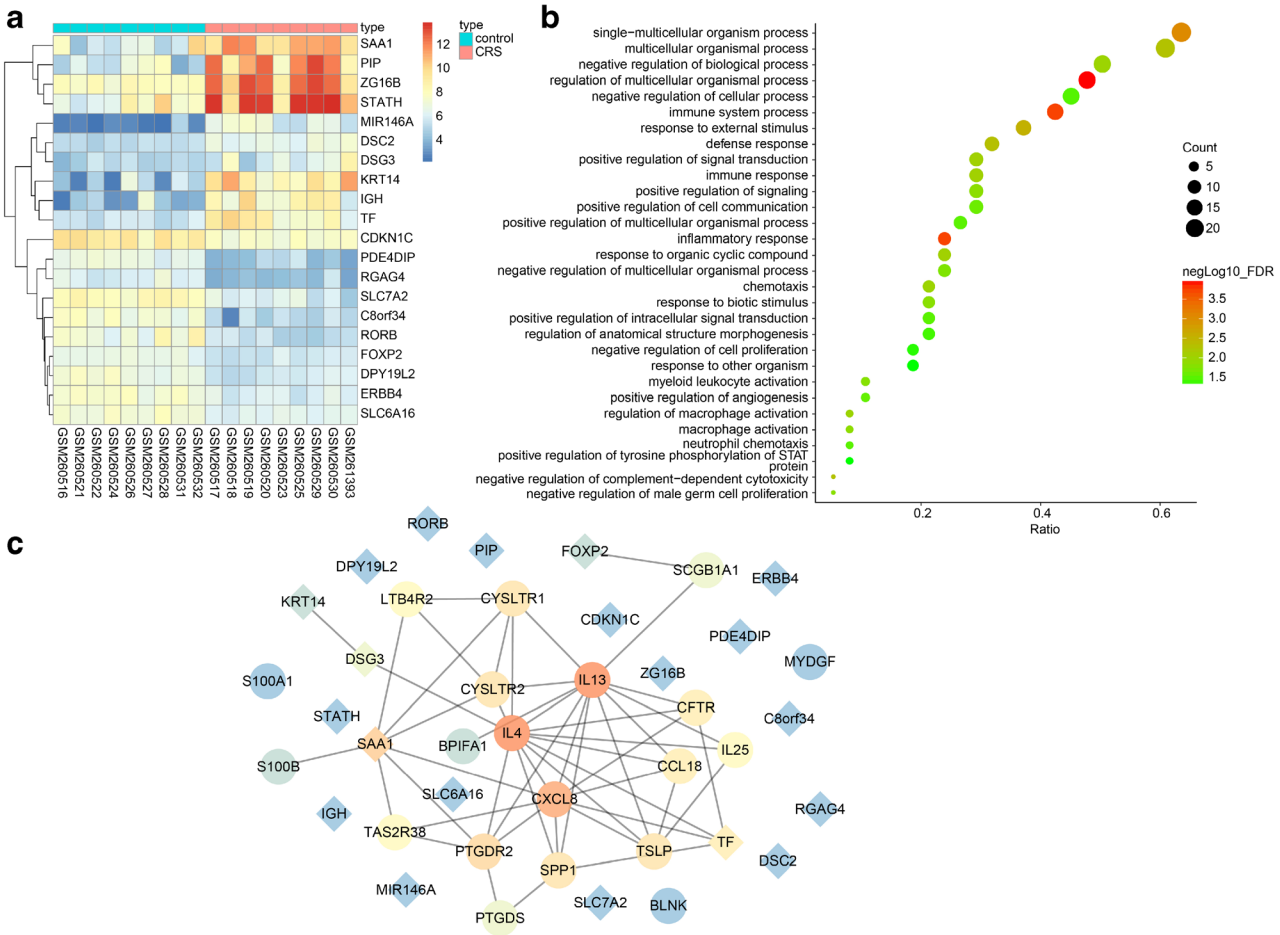


**Fig. 1.** DSG3 is selected for the study as a regulator of the Wnt/β-catenin signaling pathway. **a** The heatmap of the top 20 DEGs in GSE10406, the X-axis referring to the sample number and the Y-axis referring to the DEGs, the histogram in the upper right referring to the color gradation, and one rectangle in the graph corresponding to a gene expression value. **b** The GO enrichment analysis results of DEGs and disease genes in CRS. **c** The interaction network of DEGs and disease genes in CRS, diamonds referring to DEGs, and circles referring to disease genes. CRS chronic rhinosinusitis, DEGs differentially expressed genes, GO gene ontology.

20 genes (namely, SCGB1A1, IL13, SPP1, IL4, TSLP, CXCL8, CFTR, CYSLTR1, MYDGF, PTGDR2, BPIFA1, IL25, PTGDS, BLNK, LTB4R2, CYSLTR2, S100B, TAS2R38, CCL18, S100A1) were selected as disease-focus genes. Next, gene ontology (GO) analysis for DEGs and disease genes was conducted using the String database (Fig. 1b). The aforementioned DEGs and disease genes were found to be significantly enriched in immune response, chemotaxis, and other biological processes. These entries were recorded as the biological processes associated with sinusitis in the MalaCards database (http://www.malacards.org/), further suggesting that these DEGs and disease genes might be associated with CRS. Further, based on the gene interaction information provided by the String database, we established a network of DEGs and CRS-related genes (Fig. 1c). Several inflammatory factors were obtained with a maximum relevance to other genes in the network, such as IL13, IL4, and CXCL8. These disease genes were located at the core of the network, further indicating the significance of these genes in CRS. Additionally, TF, DSG3, and SAA1 were shown to be associated with the disease genes. A few studies have shown that the abnormal expression of DSG3 may be related to CRS [6], but the specific molecular mechanism still remains to

be unclear. According to the heatmap of the top 20 DEGs in the GSE10406 chip, the expression of DSG3 in patients with CRS was significantly higher than that in normal controls (Fig. 1a). Furthermore, activation of Wnt/β-catenin signaling pathway was demonstrated to be related to the development of CRS [12, 19]; whereas, DSG3 could affect the Wnt/β-catenin signaling pathway in cases of head neck cancer [20]. Based on the results of microarray analyses, it can be inferred that DSG3 enriched in CRS may function by regulating the Wnt/β-catenin signaling pathway, and could be further explored in search of a therapeutic target for CRS.

### CRS Mice Models Exhibit Pathological Changes in Sinus Mucosa

Hematoxylin-eosin (HE) staining was conducted in order to observe the pathological changes of the sinus mucosa of mice. In the CRS mice, the epithelial layer of the sinus mucosa was observed to be hypertrophic, and the structure of the sinus mucosa was loosened, accompanied by hyperplasia of goblet cells, epithelial cells and submucosal glands, and infiltration of a large number of eosinophils in the sub-mucosal tissues. However, the normal mice presented with intact mucosal epithelium without thickening, along with mild hyperplasia of goblet cells and few inflammatory cells. Results of AB-PAS staining showed that the CRS mice presented with purple-stained granules on the epithelial layer of the sinus mucosa; the AB-PAS staining yielded positive results, indicating obvious goblet cell hyperplasia relative to normal mice. Compared with the CRS mice, the mucosal epithelium of normal mice was observed to be slightly stained, and the AB-PAS staining yielded weakly positive or negative results (Fig. 2a–b).

### DSG3 Silencing Coupled with β-Catenin Silencing Suppresses Inflammation in Sinus Mucosa of CRS Mice Models

The expression of DSG3 and β-catenin was interfered with using siRNAs in the mice to elucidate their effects on inflammation. Subsequently, ELISA was employed in order to determine the levels of inflammatory factors TNF-α, IL-6, and IL-8 in sinus mucosa. As shown by ELISA detection results (Table 2), the levels of TNF-α, IL-6, and IL-8 were found to be increased in the sinus mucosa of mice with CRS as opposed to the normal mice (all $p < 0.05$). However, significantly decreased levels of TNF-α, IL-6, and IL-8 were observed in sinus mucosa of CRS mice treated with si-DSG3, si-β-catenin, or both of them as compared to the CRS mice without treatment ($p < 0.05$), while no significant changes were observed between CRS mice treated with NC and CRS mice without treatment ($p > 0.05$). The levels of TNF-α, IL-6, and IL-8 in the sinus mucosa of mice treated with both si-DSG3 and si-β-catenin were found to be much lower than those treated with si-DSG3 alone ($p < 0.05$), while no significant changes were observed between the CRS mice treated with si-β-catenin and si-DSG3 ($p > 0.05$). The aforementioned results revealed that the release of pro-inflammatory factors could be reduced by silencing DSG3 and β-catenin expression in CRS mice.

### DSG3 and β-Catenin Silencing Decreases the Positive Rates of MUC5B and MUC5AC

Additionally, immunohistochemical staining was employed in order to measure the positive rate of MUC5B and MUC5AC. In the sinus mucosa of CRS mice, MUC5B was observed to be partially expressed in the cytoplasm and in the membrane of epithelial cells, as noted by brown staining. MUC5A was stained with brown coloration, strongly and positively expressed in epithelial cells, and primarily expressed in goblet cells (Fig. 3a, b). Compared with the normal mice, the positive rates of MUC5B and MUC5AC were found to be increased in CRS mice ($p < 0.05$). The positive rates of MUC5B and MUC5AC in the CRS mice treated with si-DSG3, si-β-catenin, or both of them were all lower than that in the CRS mice without treatment ($p < 0.05$). No significant changes were visualized in the positive rates of MUC5B and MUC5AC between the CRS mice without treatment and CRS mice treated with NC ($p > 0.05$). However, the combined treatment of si-DSG3 and si-β-catenin contributed to declines in the positive rates of MUC5B and MUC5AC when compared to individual si-DSG3 treatment ($p < 0.05$), whereas there were no remarkable differences between the mice treated with si-β-catenin and si-DSG3 ($p > 0.05$) (Fig. 3c). The results suggest that the positive expression of MUC5B and MUC5AC could be reduced by silencing both DSG3 and β-catenin.

### DSG3 and β-Catenin Silencing Increases the Apoptosis of Goblet Cells

TUNEL staining was conducted in order to examine the apoptosis rates of goblet cells, and the results (Fig. 4a–b) showed decreased apoptosis rates of goblet cells in CRS mice in comparison with the normal mice (all $p < 0.05$). In comparison to the CRS mice without

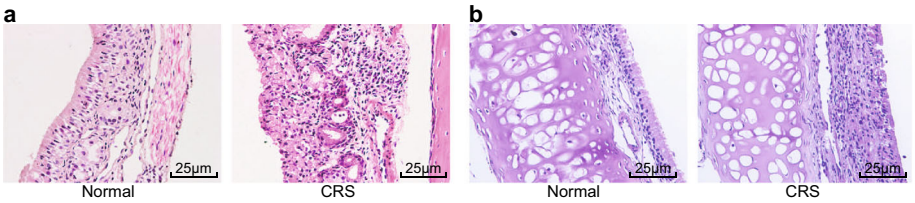


**Fig. 2.** Observation of pathological changes of sinus mucosa in CRS mice models. **a** HE staining of sinus mucosa in normal mice and mice of CRS model (400×). **b** AB-PAS staining of sinus mucosa in normal mice and mice of CRS model (400×). CRS chronic rhinosinusitis, HE staining hematoxylin-eosin staining, AB-PAS staining Alcian blue-periodic acid-Schiff staining.

treatment, the apoptosis rate of goblet cells was found to be increased in the CRS mice treated with si-DSG3, si-β-catenin, or both of them ($p < 0.05$), while there were no significant changes in the apoptosis rate of goblet cells between the CRS mice without treatment and CRS mice treated with NC ($p > 0.05$). The apoptosis rate of goblet cells in the CRS mice treated with si-DSG3 plus si-β-catenin was found to be increased compared to individual si-DSG3 treatment ($p < 0.05$), whereas there were no remarkable differences demonstrated in the apoptosis rate of goblet cells between the mice treated with si-β-catenin and si-DSG3 ($p > 0.05$). The results suggest that silencing both DSG3 and β-catenin could enhance the apoptosis of goblet cells.

### The Wnt/β-Catenin Signaling Pathway Is Disrupted by Depression of DSG3

RT-qPCR and Western blot analysis were employed in order to determine the mRNA and protein levels of DSG3, Wnt, β-catenin, and GSK3β in the sinus mucosa of mice. The results revealed that the mRNA and protein levels of DSG3, Wnt, and β-catenin in the CRS mice were increased while those of GSK3β were decreased compared to the normal mice ($p < 0.05$). As compared to the CRS mice without treatment, the mRNA and protein levels of DSG3, Wnt, and β-catenin in the CRS mice treated with si-DSG3 or both si-DSG3 and si-β-catenin were remarkably reduced while those of GSK3β were dramatically elevated ($p < 0.05$). There were no obvious changes in the mRNA and protein levels of related genes in CRS mice without treatment and CRS mice treated with NC ($p > 0.05$). Whereas, the mRNA and protein levels of DSG3 were found to be unchanged, while those of Wnt, β-catenin were significantly reduced, and those of GSK3β were significantly increased in the CRS mice treated with si-β-catenin when compared to that in CRS mice without treatment ($p < 0.05$). Compared with the CRS mice treated with si-DSG3, there were no significant changes in the mRNA and protein levels of DSG3 ($p > 0.05$), while the mRNA and protein levels of Wnt and β-catenin were markedly reduced, and those of GSK3β were significantly increased in the CRS mice treated with both si-DSG3 and si-β-catenin ($p < 0.05$). The mRNA and protein levels of DSG3 were increased ($p < 0.05$), and the mRNA and protein levels of Wnt, β-catenin, and GSK3β showed no significant differences in the CRS mice treated with si-DSG3 and si-β-catenin ($p > 0.05$) (Fig. 5a–c). Taken together, the results suggest that the mRNA and protein levels of Wnt and β-catenin were

**Table 2.** Both DSG3 silencing and β-catenin silencing reduce the levels of pro-inflammatory factors

| Group | TNF-α (pg/mL) | IL-6 (pg/mL) | IL-8 (pg/mL) |
|---|---|---|---|
| Normal | 1.35 ± 0.13 | 28.82 ± 3.04 | 286.79 ± 52.71 |
| CRS | 6.56 ± 1.53* | 110.93 ± 15.38* | 884.60 ± 101.34* |
| NC | 6.02 ± 1.26* | 107.63 ± 13.92* | 863.38 ± 83.29* |
| si-DSG3 | 4.38 ± 0.72*# | 78.83 ± 11.93*# | 698.47 ± 58.91*# |
| si-β-catenin | 4.11 ± 1.13*# | 80.03 ± 12.03*# | 650.38 ± 55.83*# |
| si-DSG3 + si-β-catenin | 2.73 ± 0.57*#& | 53.24 ± 6.89*#& | 428.46 ± 73.24*#& |

* $p < 0.05$ *vs.* the normal group; # $p < 0.05$ *vs.* the CRS group; & $p < 0.05$ *vs.* the si-DSG3 group; the results of ELISA assay were measurement data expressed as mean ± standard deviation, and the comparison of data among multiple groups was analyzed by one-way variance analysis, $n = 10$. *ELISA* enzyme-linked immunosorbent assay, *CRS* chronic rhinosinusitis, *NC* negative control, *DSG3* desmoglein 3, *TNF-α* tumor necrosis factor, *IL* interleukin

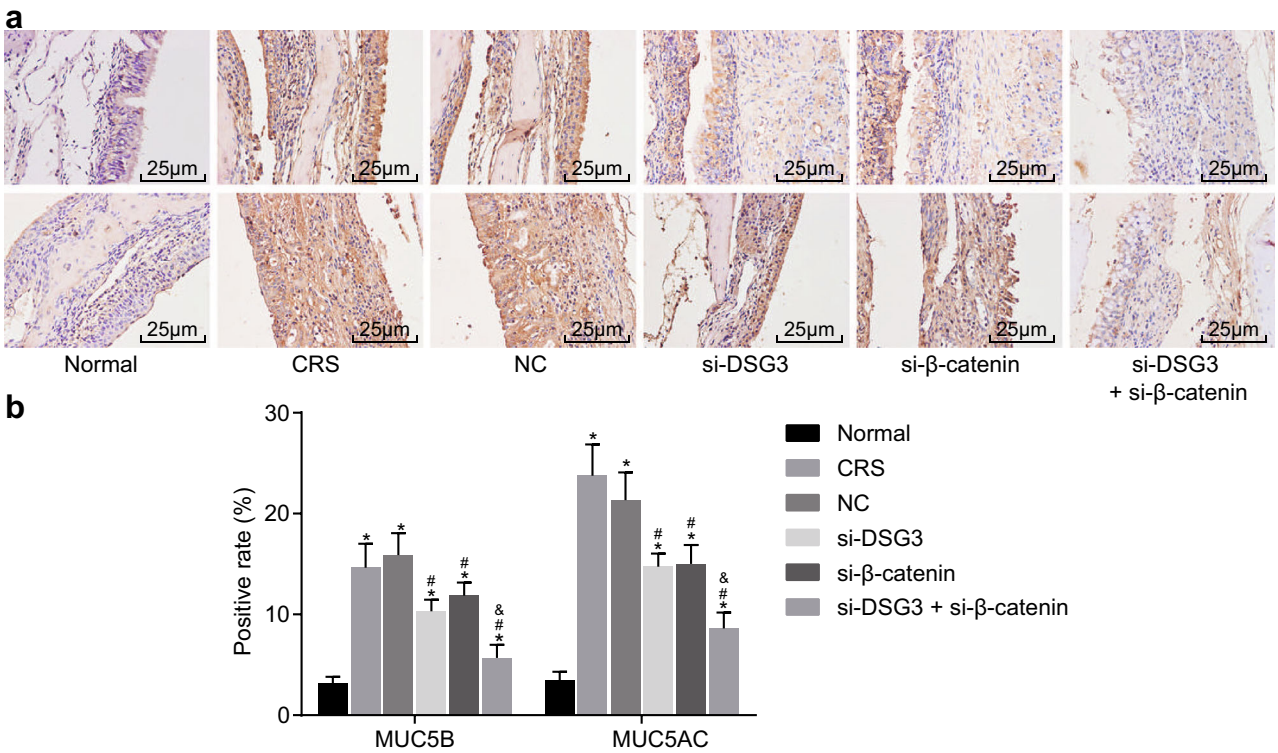


**Fig. 3.** Suppression of both DSG3 and β-catenin reduces the positive expression of MUC5B and MUC5AC. **a** Positive expression of MUC5B in sinus mucosa of mice detected by immunohistochemical staining (400×). **b** Positive expression of MUC5AC in sinus mucosa of mice detected by immunohistochemical staining (400×). **c** Positive rates of MUC5B and MUC5AC in sinus mucosa of mice after alternation of DSG3 and β-catenin expression; $^{*}p < 0.05$ *vs.* the normal group; $^{\#}p < 0.05$ *vs.* the CRS group; $^{\&}p < 0.05$ *vs.* the si-DSG3 group; in the immunohistochemical staining, cells stained with brown coloration were considered as positive cells. Measurement data expressed as mean ± standard deviation. Data among multiple groups were compared by one-way analysis of variance ($n = 10$). CRS chronic rhinosinusitis, NC negative control, DSG3 desmoglein 3, MUC5B mucin 5B, MUC5AC mucin 5 AC.

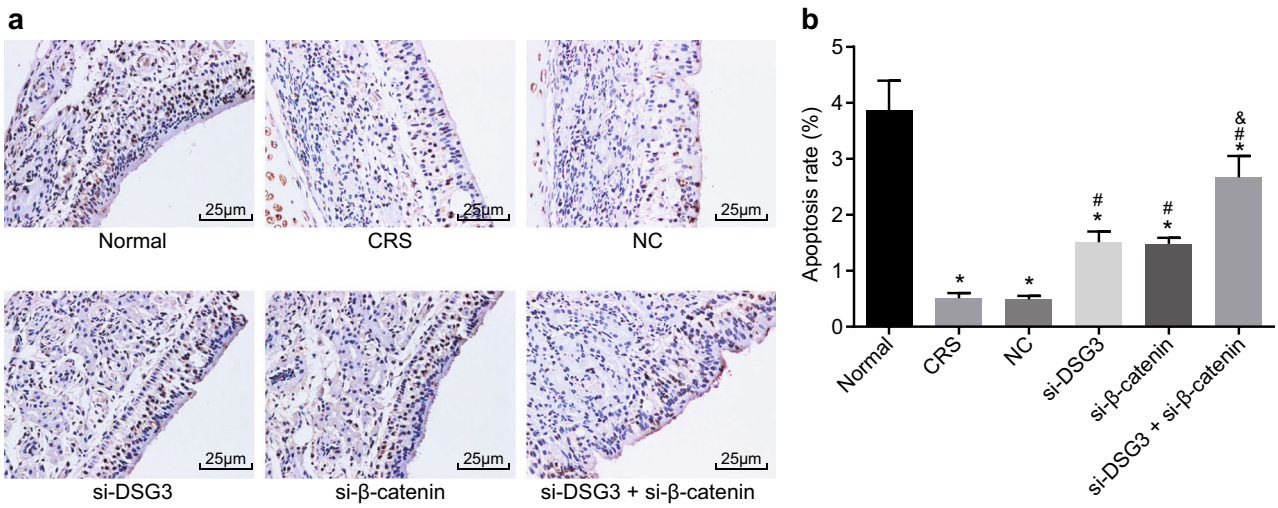


**Fig. 4.** Downregulated expression of DSG3 and β-catenin increases the apoptosis of goblet cells. **a** TUNEL staining of the goblet cells in the sinus mucosa of all the mice. **b** The apoptosis rate of the goblet cells in sinus mucosa of the mice in response to alternation of DSG3 and β-catenin expression. $^{*}p < 0.05$ *vs.* the normal group; $^{\#}p < 0.05$ *vs.* the CRS group; $^{\&}p < 0.05$ *vs.* the si-DSG3 group; the results of apoptosis were expressed by mean ± standard deviation. The cell apoptosis in each group was analyzed by one-way analysis of variance. CRS chronic rhinosinusitis, NC negative control, DSG3 desmoglein 3, TUNEL terminal deoxynucleotidyl transferase (TdT)-mediated dUTP nick-end labeling.

decreased but those of GSK3β were enhanced by silencing of depression of DSG3.

## DISCUSSION

CRS is deemed as a persistent state of inflammation in the nasal and paranasal sinuses for a minimum duration of 12 weeks [21]. Previously, a study focusing on CRS demonstrated that the mRNA and protein expression of DSG3 were increased in the sinus mucosa of CRS arrays [6]. Consistently, DSG3 was also found to be expressed at a high level in CRS in the current study. Our findings provided evidence about the effects of DSG3 on the inflammatory response in CRS through regulation of the Wnt/β-catenin signaling pathway. In mice models of CRS, the suppression of DSG3 contributed to a decreased inflammatory response and goblet cell mucin secretion *via* inhibition of the Wnt/β-catenin signaling pathway.

In the mice of CRS model, DSG3 silencing and β-catenin silencing downregulated the release of inflammatory factors TNF-α, IL-6, and IL-8 in the sinus mucosa. DSG3 played a major role in preserving epidermal integrity, which was found to be involved in autoimmune skin inflammation [7, 22]. Moreover, epidermal DSG3 could be recognized by Th17 cells carrying TCR so as to induce psoriasis-like skin inflammation and develop cutaneous psoriasis-like immunopathology [23]. Furthermore, in most cases, the pathogenesis of autoimmune inflammation correlates with the levels of cytokines, TNF-α and IL-6, two important pro-inflammatory cytokines [24]. After *Staphylococcus aureus* induced CRS in mice, the expression of pro-inflammatory cytokines (TNF-α, IL-6, and IL-8) was observed to be increased, which indicates their importance in the pathogenesis of CRS. Moreover, the protective role of TNF-α in chemical-induced breast cancer carcinogenesis through its function over inflammation has been previously proved [25]. Inflammatory activities in CRS are modulated typically by pro-inflammatory cytokines that distributed locally in sinonasal tissues, such as TNF-α and IL-6, which are correlated with the suppression of olfactory function [26]. Additionally, the current study found that the expression of inflammatory factors TNF-α, IL-1β, and IL-6 was downregulated by silencing DSG3 and β-catenin. Similarly, transcription factor nuclear factor kappa-B (NF-κB) was previously revealed to participate in the process of inflammatory response owing to its role in the induction of inflammatory factor transcription [27]. Interestingly, it has been found that silencing of β-catenin was able to reduce lipopolysaccharide-induced NF-κB activation and the expression of pro-inflammatory cytokines (TNF-α, IL-6, and IL-8) in human bronchial epithelial cells [28]. Furthermore, after cell culture with antibody to DSG3, increased mRNA expression of IL-1β, TNF-α, and IL-6 was noted, which validates their role in pathogenesis of pemphigus vulgaris and is in line with the trend of the current study [29].

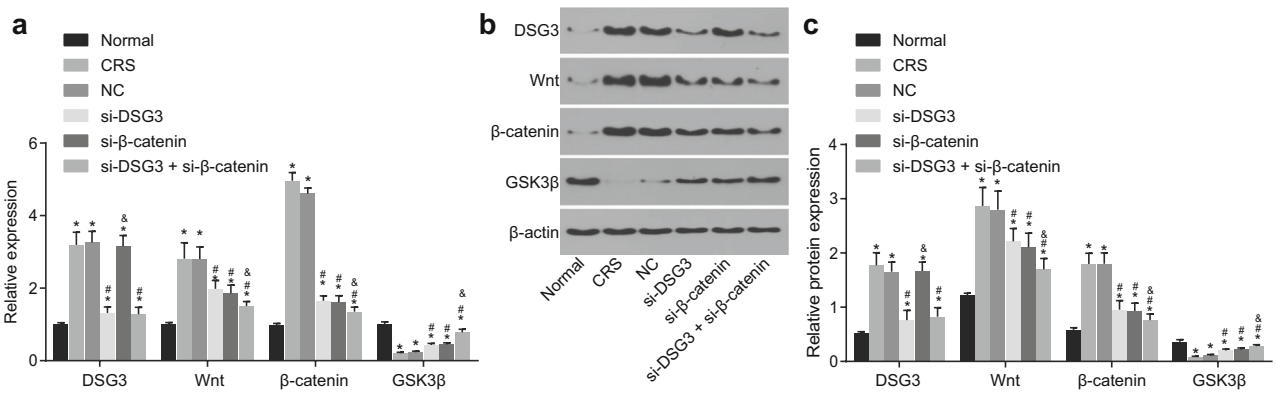


**Fig. 5.** The loss of DSG3 by siRNA silencing blocks activation of the Wnt/β-catenin signaling pathway. **a** The mRNA expression of DSG3, Wnt, β-catenin, and GSK3β in the sinus mucosa of mice determined by RT-qPCR. **b** Protein bands of DSG3, Wnt, β-catenin, and GSK3β in the sinus mucosa of mice measured by Western blot analysis. **c** The relative protein expression of DSG3, Wnt, β-catenin, and GSK3β in the sinus mucosa of mice in each group. $^{*}p < 0.05$ *vs.* the normal group; $^{\#}p < 0.05$ *vs.* the CRS group; $^{\&}p < 0.05$ *vs.* the si-DSG3 group; the results of RT-qPCR and Western blot analysis were measurement data expressed as the mean ± standard deviation. Data among multiple groups were compared using one-way analysis of variance, $n = 10$. CRS chronic rhinosinusitis, NC negative control, DSG3 desmoglein 3, GSK3β glycogen synthase kinase-3β.

The current study further employed immunohistochemical and TUNEL staining regimens, and the secretions of MUC5B and MUC5AC were noted to be reduced in goblet cells, whereas the apoptosis rate of goblet cells was increased as a result of silencing DSG3 or β-catenin. Specifically, the mucin MUC5AC, a critical part of respiratory tract mucus, was previously demonstrated to be associated with respiratory disease susceptibility [30]. MUC5B is the main mucin in the healthy mucus secretions of mice, which confers for congenital defense in the upper and lower airways [31]. Coincidently, CRS is a type of mucus hypersecretion disease, and exhibits upregulated expression of MUC5AC and MUC5B [32, 33]. DSG3 and MUC1 were both regarded as biomarkers for idiopathic interstitial pneumonias, and both were found to be upregulated in idiopathic interstitial pneumonias [34]. Goblet cells in the surface epithelium and mucous and serous cells could secrete mucin glycoproteins, which maintain normal homeostasis through regulating mucosal innate immune responses [6]. Furthermore, a previous study revealed that downregulation of MUC5B can alter the activation of the Wnt/β-catenin signaling pathway so to inhibit tumor growth [35]. Moreover, the Wnt/β-catenin signaling pathway is known to be associated with diminished goblet cell metaplasia [36].

By means of RT-qPCR and Western blot analysis, we discovered that the mRNA and protein expression of DSG3, Wnt, and β-catenin was decreased in sinus mucosa, while those of GSK3β were raised as a result of silencing DSG3. GSK3β, an inhibitor of the Wnt/β-catenin signaling pathway, was revealed to decreases the expression of MUC5AC in an allergic airway disease model [36]. In addition, the cytoplasmic ligand of DSG3 was found to be involved in cell signaling which is similar to the β-catenin signaling pathway, acting as a tumor suppressor [37]. DSG3 played a crucial role in cell–cell adhesion through mediation of membrane trafficking of cadherins, which was implicated in β-catenin-dependent transcription [38, 39]. However, more research is warranted to explain the possible interactions between DSG3, cadherins, and β-catenin.

## CONCLUSION

In conclusion, the current study suggests the effect of downregulated DSG3 on reducing inflammatory response and goblet cell mucin secretion of mice with CRS through suppression of the Wnt/β-catenin signaling pathway. These findings may open novel avenues for future CRS therapeutic regimens. It should be noted that this study only examined the goblet cell apoptosis in mice with CRS, without performing epithelial cell experiments. A more comprehensive investigation about the effects on other inflammatory factors should be conducted in the future, and clinical data should be provided to support the results.

## ACKNOWLEDGEMENTS

We acknowledge and appreciate our colleagues for their valuable efforts and comments on this paper.

## FUNDING INFORMATION

This work is supported by Medical and Health Project of Jilin Science and Technology Development Plan (No. 20190304037YY).

## COMPLIANCE WITH ETHICAL STANDARDS

**Competing Interests.** The authors declare that they have no conflict of interest.

## REFERENCES

1. Thompson, G.R., 3rd, and T.F. Patterson. 2012. Fungal disease of the nose and paranasal sinuses. *The Journal of Allergy and Clinical Immunology* 129 (2): 321–326.
2. Kern, R.C., J.P. Stolovitzky, S.L. Silvers, A. Singh, J.T. Lee, D.M. Yen, A.M.C. Iloreta Jr., F.P.J. Langford, B. Karanfilov, K.E. Matheny, J.W. Stambaugh, A.K. Gawlicka, and investigators, R.I.s. 2018. A phase 3 trial of mometasone furoate sinus implants for chronic sinusitis with recurrent nasal polyps. *International Forum of Allergy and Rhinology* 8 (4): 471–481.
3. Tan, L., A. Psaltis, L.M. Baker, M. McGuckin, K. Rousseau, and P.J. Wormald. 2010. Aberrant mucin glycoprotein patterns of chronic rhinosinusitis patients with bacterial biofilms. *American Journal of Rhinology & Allergy* 24 (5): 319–324.
4. Zhang, Y., E. Gevaert, H. Lou, X. Wang, L. Zhang, C. Bachert, and N. Zhang. 2017. Chronic rhinosinusitis in Asia. *The Journal of Allergy and Clinical Immunology* 140 (5): 1230–1239.
5. Karunasagar, A., S.S. Garag, S.B. Appannavar, R.D. Kulkarni, and A.S. Naik. 2018. Bacterial biofilms in chronic rhinosinusitis and their implications for clinical management. *Indian Journal of Otolaryngology and Head and Neck Surgery : Official Publication of the Association of Otolaryngologists of India* 70 (1): 43–48.
6. Wu, X., J.R. Peters-Hall, S. Ghimbovschi, R. Mimms, M.C. Rose, and M.T. Pena. 2011. Glandular gene expression of sinus

mucosa in chronic rhinosinusitis with and without cystic fibrosis. *American Journal of Respiratory Cell and Molecular Biology* 45 (3): 525–533.
7. Kitashima, D.Y., T. Kobayashi, T. Woodring, K. Idouchi, T. Doebel, B. Voisin, T. Adachi, T. Ouchi, H. Takahashi, K. Nishifuji, D.H. Kaplan, B.E. Clausen, M. Amagai, and K. Nagao. 2018. Langerhans cells prevent autoimmunity via expansion of keratinocyte antigen-specific regulatory T cells. *EBioMedicine* 27: 293–303.
8. Tsang, S.M., L. Brown, K. Lin, L. Liu, K. Piper, E.A. O'Toole, R. Grose, I.R. Hart, D.R. Garrod, F. Fortune, and H. Wan. 2012. Non-junctional human desmoglein 3 acts as an upstream regulator of Src in E-cadherin adhesion, a pathway possibly involved in the pathogenesis of pemphigus vulgaris. *The Journal of Pathology* 227 (1): 81–93.
9. Gama, A., and F. Schmitt. 2012. Cadherin cell adhesion system in canine mammary cancer: A review. *Veterinary Medicine International* 2012: 357187.
10. Lu, T.L., and C.M. Chen. 2015. Beta-catenin in epithelial tumorigenesis. *Aging (Albany NY)* 7 (7): 467–468.
11. Ma, H., W. Li, P. Bi, Q. Wang, J. Li, and B. Yang. 2018. hsa-miR-93 regulates MUCIN family gene expression via WNT/beta-catenin pathway in intrahepatic stone disease. *Clinics and Research in Hepatology and Gastroenterology* 42 (5): 453–461.
12. Boscke, R., E.K. Vladar, M. Konnecke, B. Husing, R. Linke, R. Pries, N. Reiling, J.D. Axelrod, J.V. Nayak, and B. Wollenberg. 2017. Wnt signaling in chronic rhinosinusitis with nasal polyps. *American Journal of Respiratory Cell and Molecular Biology* 56 (5): 575–584.
13. Rotzer, V., E. Hartlieb, F. Vielmuth, M. Gliem, V. Spindler, and J. Waschke. 2015. E-cadherin and Src associate with extradesmosomal Dsg3 and modulate desmosome assembly and adhesion. *Cellular and Molecular Life Sciences* 72 (24): 4885–4897.
14. Ahn, S.K., S.Y. Jeon, R. Khalmuratov, D.J. Kim, J.P. Kim, J.J. Park, and D.G. Hur. 2008. Rat model of staphylococcal enterotoxin B-induced rhinosinusitis. *Clinical and Experimental Otorhinolaryngology* 1 (1): 24–28.
15. Hoshino, M., Y. Fujita, J. Saji, T. Inoue, T. Nakagawa, and T. Miyazawa. 2005. Effect of suplatast tosilate on goblet cell metaplasia in patients with asthma. *Allergy* 60 (11): 1394–1400.
16. Qin, Z., X. Li, X. Cai, J. Li, H. Zhu, Y. Ma, S. Wu, D. Liu, and X. Li. 2016. Periostin: A novel biomarker for chronic rhinosinusitis. *B-ENT* 12 (4): 305–313.
17. Maxfield, A.Z., L.D. Landegger, C.D. Brook, A.E. Lehmann, A.P. Campbell, R.W. Bergmark, K.M. Stankovic, and R. Metson. 2018. Periostin as a biomarker for nasal polyps in chronic rhinosinusitis. *Otolaryngology and Head and Neck Surgery* 158 (1): 181–186.
18. Zhong, H., A.M. De Marzo, E. Laughner, M. Lim, D.A. Hilton, D. Zagzag, P. Buechler, W.B. Isaacs, G.L. Semenza, and J.W. Simons. 1999. Overexpression of hypoxia-inducible factor 1alpha in common human cancers and their metastases. *Cancer Research* 59 (22): 5830–5835.
19. Wu, J., W. Kong, and Y. Yu. 2010. Up-regulation of Wnt5A in chronic rhinosinusitis with nasal polyps. *Lin Chung Er Bi Yan Hou Tou Jing Wai Ke Za Zhi* 24 (23): 1064–1067.
20. Chen, Y.J., L.Y. Lee, Y.K. Chao, J.T. Chang, Y.C. Lu, H.F. Li, C.C. Chiu, Y.C. Li, Y.L. Li, J.F. Chiou, and A.J. Cheng. 2013. DSG3 facilitates cancer cell growth and invasion through the DSG3-plakoglobin-TCF/LEF-Myc/cyclin D1/MMP signaling pathway. *PLoS One* 8 (5): e64088.
21. Koennecke, M., F. Benecke, A. Masche, R. Linke, K.L. Bruchhage, R. Pries, L. Klimek, and B. Wollenberg. 2018. Increased phosphorylation of eNOS in nasal polyps of chronic rhinosinusitis patients can be diminished by 1,8-cineol. *Nitric Oxide* 78: 89–94.
22. Nishimura, H., and J.L. Strominger. 2006. Involvement of a tissue-specific autoantibody in skin disorders of murine systemic lupus erythematosus and autoinflammatory diseases. *Proceedings of the National Academy of Sciences of the United States of America* 103 (9): 3292–3297.
23. Nishimoto, S., H. Kotani, S. Tsuruta, N. Shimizu, M. Ito, T. Shichita, R. Morita, H. Takahashi, M. Amagai, and A. Yoshimura. 2013. Th17 cells carrying TCR recognizing epidermal autoantigen induce psoriasis-like skin inflammation. *Journal of Immunology* 191 (6): 3065–3072.
24. Moudgil, K.D., and D. Choubey. 2011. Cytokines in autoimmunity: Role in induction, regulation, and treatment. *Journal of Interferon & Cytokine Research* 31 (10): 695–703.
25. Storci, G., P. Sansone, S. Mari, G. D'Uva, S. Tavolari, T. Guarnieri, M. Taffurelli, C. Ceccarelli, D. Santini, P. Chieco, K.B. Marcu, and M. Bonafe. 2010. TNF alpha up-regulates SLUG via the NF-kappaB/HIF1alpha axis, which imparts breast cancer cells with a stem cell-like phenotype. *Journal of Cellular Physiology* 225 (3): 682–691.
26. Wu, J., R.K. Chandra, P. Li, B.P. Hull, and J.H. Turner. 2018. Olfactory and middle metal cytokine levels correlate with olfactory function in chronic rhinosinusitis. *Laryngoscope* 128 (9): E304–E310.
27. Wee, J.H., Y.L. Zhang, C.S. Rhee, and D.Y. Kim. 2017. Inhibition of allergic response by intranasal selective NF-kappaB decoy oligodeoxynucleotides in a murine model of allergic rhinitis. *Allergy, Asthma & Immunology Research* 9 (1): 61–69.
28. Jang, J., J.H. Ha, S.I. Chung, and Y. Yoon. 2014. Beta-catenin regulates NF-kappaB activity and inflammatory cytokine expression in bronchial epithelial cells treated with lipopolysaccharide. *International Journal of Molecular Medicine* 34 (2): 632–638.
29. Narbutt, J., J. Boncela, K. Smolarczyk, C. Kowalewski, K. Wozniak, J.D. Torzecka, A. Sysa-Jedrzejowska, C.S. Cierniewski, and A. Lesiak. 2012. Pathogenic activity of circulating anti-desmoglein-3 autoantibodies isolated from pemphigus vulgaris patients. *Archives of Medical Science* 8 (2): 347–356.
30. Johnson, L., I. Shah, A.X. Loh, L.E. Vinall, A.S. Teixeira, K. Rousseau, J.W. Holloway, R. Hardy, and D.M. Swallow. 2013. MUC5AC and inflammatory mediators associated with respiratory outcomes in the British 1946 birth cohort. *Respirology* 18 (6): 1003–1010.
31. Evans, C.M., M.A. Seibold, and A.N. Gerber. 2018. SPDEFending the lung through mucin expression. *American Journal of Respiratory Cell and Molecular Biology* 59 (3): 287–288.
32. Luo, Q., H. Zhu, K. Feng, X. Huang, X. Jing, and J. Zhang. 2015. Expression of hypoxia inducible factor-1alpha in chronic rhinosinusitis and the relationship with mucin secretion. *Zhonghua Er Bi Yan Hou Tou Jing Wai Ke Za Zhi* 50 (2): 138–144.
33. Luo, Q., J. Zhang, H. Wang, F. Chen, X. Luo, B. Miao, X. Wu, R. Ma, X. Luo, G. Xu, J. Shi, and H. Li. 2015. Expression and regulation of transcription factor FoxA2 in chronic rhinosinusitis with and without nasal polyps. *Allergy, Asthma & Immunology Research* 7 (5): 458–466.
34. Horimasu, Y., N. Ishikawa, M. Taniwaki, K. Yamaguchi, K. Hamai, H. Iwamoto, S. Ohshimo, H. Hamada, N. Hattori, M. Okada, K. Arihiro, Y. Ohtsuki, and N. Kohno. 2017. Gene expression profiling of idiopathic interstitial pneumonias (IIPs): Identification of potential diagnostic markers and therapeutic targets. *BMC Medical Genetics* 18 (1): 88.
35. Lahdaoui, F., M. Messager, A. Vincent, F. Hec, A. Gandon, M. Warlaumont, F. Renaud, E. Leteurtre, G. Piessen, N. Jonckheere, C. Mariette, and I. Van Seuningen. 2017. Depletion of MUC5B

mucin in gastrointestinal cancer cells alters their tumorigenic properties: Implication of the Wnt/beta-catenin pathway. *The Biochemical Journal* 474 (22): 3733–3746.
36. Reuter, S., H. Beckert, and C. Taube. 2016. Take the Wnt out of the inflammatory sails: Modulatory effects of Wnt in airway diseases. *Laboratory Investigation* 96 (2): 177–185.
37. Kyrodimou, M., D. Andreadis, A. Drougou, E.P. Amanatiadou, L. Angelis, C. Barbatis, A. Epivatianos, and I.S. Vizirianakis. 2014. Desmoglein-3/gamma-catenin and E-cadherin/ss-catenin differential expression in oral leukoplakia and squamous cell carcinoma. *Clinical Oral Investigations* 18 (1): 199–210.
38. Moftah, H., K. Dias, E.H. Apu, L. Liu, J. Uttagomol, L. Bergmeier, S. Kermorgant, and H. Wan. 2017. Desmoglein 3 regulates membrane trafficking of cadherins, an implication in cell-cell adhesion. *Cell Adhesion & Migration* 11 (3): 211–232.
39. Howard, S., T. Deroo, Y. Fujita, and N. Itasaki. 2011. A positive role of cadherin in Wnt/beta-catenin signalling during epithelial-mesenchymal transition. *PLoS One* 6 (8): e23899.